Particle-based modeling of oxygen discharges

F. X. Bronold[1], K. Matyash[2], David Tskhakaya[3], Ralf Schneider[2], and Holger Fehske[1]

[1] *Institut für Physik, Ernst-Moritz-Arndt-Universität Greifswald, D-17489 Greifswald*
[2] *Max-Planck-Institut für Plasmaphysik, Teilinstitut Greifswald, D-17491 Greifswald*
[3] *Institut für Theoretische Physik, Universität Innsbruck, A-6020 Innsbruck, Österreich*

We present an one-dimensional particle-in-cell Monte-Carlo model for capacitively coupled radio-frequency discharges in oxygen. The model quantitatively describes the central part of the discharge. For a given voltage and pressure, it self-consistently determines the electric potential and the distribution functions for electrons, negatively charged atomic oxygen, and positively charged molecular oxygen. Previously used collision cross sections are critically assessed and in some cases modified. Provided associative detachment due to metastable oxygen molecules is included in the model, the electro-negativities in the center of the discharge are in excellent agreement with experiments. Due to lack of empirical data for the cross section of this process, we propose a simple model and discuss its limitations.

1. Introduction

Discharges in reactive gases such as oxygen play an important role in plasma-assisted etching and thin-film deposition techniques. The requirements on the controllability and reliability of these discharges are so high, that further advancement of this technology critically depends on improved descriptions of the physical processes. In particular, the interplay between the macroscopic electrodynamics, which is used to control the discharge, and the microscopic plasma-chemical processes, which sustain the discharge and give rise to the materials processing, has to be understood not only qualitatively but quantitatively.

Particle-based modeling is well suited for this task, because it directly simulates the Boltzmann-Poisson system describing the discharge without any assumptions concerning the species' distribution functions or the electric field. Provided the elementary plasma-chemical processes are well characterized in terms of cross sections, they can be easily incorporated in the collision integral of the Boltzmann equation. Through the source term of the Poisson equation, the plasma-chemistry is then linked to the electrodynamics of the discharge.

In the following we give a brief account of our implementation of the particle-in-cell Monte-Carlo collision (PIC-MCC) approach for the modeling of capacitively coupled radio-frequency (rf) discharges in oxygen. Our main focus will be the critical assessment of cross section data for (O_2^+, O_2) charge exchange scattering, ion-ion neutralization, and detachment due to metastables. A full description of our approach, whose treatment of collisions is closely related to the direct simulation Monte-Carlo approach for rarefied gases, will be given elsewhere [1].

2. Model

The description of an oxygen discharge could be based on a brute force numerical solution of the Boltzmann-Poisson system which couples the distribution functions of the relevant species with the electric potential. In most cases, however, this approach is not practical. More promising are methods which track the spatio-temporal evolution of a sample of pseudo-particles subject to elastic, inelastic, and reactive collisions. These approaches are based on the decoupling of collisions from the free flights in the self-consistent electric field. When the cross sections for the collisions are known, the durations of the free flights, as well as the probability for a collision of a particular type to occur, can be simply obtained from elementary kinetic considerations.

Our simulations of capacitively coupled rf discharges in oxygen [2,3] are restricted to the central axial part of the reactor (see Fig. 1). Ignoring the (electric) asymmetry between the grounded and powered electrode, we use an one-dimensional (1D) model, which keeps only one spatial coordinate, $0 \le x \le L$, where L is the distance between the electrodes, but retains all three velocity coordinates $v_x, v_y,$ and v_z. One of the electrodes is electrically driven by a time-dependent volt-
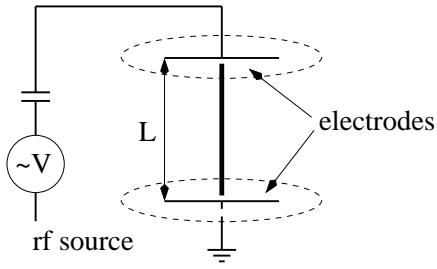
Fig. 1: Schematic geometry of the rf discharges used in Refs. [2, 3]. We use an 1D model to simulate the central axial part of the discharge (thick solid line).

age, $U_{\mathrm{rf}}(t) = U \sin 2\pi f$, while the other is set to $U = 0$. Both electrodes are totally absorbing, secondary electron emission is neglected, and the oxygen molecules are treated as an inexhaustible reservoir, the density of which is $n_{O_2} = p/kT$, where $T = 300\ K$ and p is the gas pressure.

The complex plasma-chemistry of oxygen gives rise to a large variety of collisions. In Table 1 we show the ones with the largest cross sections. They are included in our model. We simulate only three species: electrons (e), negatively charged atomic oxygen (O^-), and positively charged molecular oxygen (O_2^+). Neutral particles are not treated kinetically. They are only accounted for in as far as their production leads to an energy loss for electrons (collisions (10)–(15)) and in as far as they affect the balance of simulated particles (reactions (16)–(22)).

Our collection of cross sections is semi-empirical, combining measured data with models for the low-energy asymptotic. A complete discussion of the molecular physics entering the simulation will be given elsewhere [1]. Here it suffices to mention that the cross sections for (O_2, O_2^+) charge exchange scattering (9), ion-ion neutralization (17), and detachment (19,20) significantly deviate from the ones used previously [4] (see Fig. 2). Our simulations indicate that the modifications are essential for obtaining results in accordance with experiments [2,3].

Using $\sigma_{cx}(E) = \sigma_m(E)/2$, where σ_m and σ_{cx} denote, respectively, the momentum and charge exchange cross section, and E is the relative kinetic energy, we based our cross section for (O_2, O_2^+) charge exchange scattering below 0.251 eV and above 8.5 eV on empirical data for momentum scattering [5, 6]. For energies in between, we employed a linear interpolation. With this cross section, we obtained O_2^+ velocity distri-

Table 1: Elastic, inelastic, and reactive collisions included in our model [1].

elastic scattering
(1) $e + e \to e + e$
(2) $O^- + O^- \to O^- + O^-$
(3) $O_2^+ + O_2^+ \to O_2^+ + O_2^+$
(4) $e + O_2^+ \to e + O_2^+$
(5) $e + O^- \to e + O^-$
(6) $O^- + O_2^+ \to O^- + O_2^+$
(7) $e + O_2 \to e + O_2$
(8) $O^- + O_2 \to O^- + O_2$
(9) $O_2^+ + O_2 \to O_2 + O_2^+$
electron energy loss scattering
(10) $e + O_2 \to e + O_2(\nu = 1, ..., 4)$
(11) $e + O_2 \to e + O_2(\mathrm{Ryd})$
(12) $e + O_2 \to e + O(3P) + O(3P)$ (6.4 eV)
(13) $e + O_2 \to e + O(3P) + O(1D)$ (8.6 eV)
(14) $e + O_2 \to e + O_2(a^1\Delta_g)$
(15) $e + O_2 \to e + O_2(b^1\Sigma_g)$
electron & ion production & loss
(16) $e + O_2^+ \to O + O$
(17) $O^- + O_2^+ \to O + O_2$
(18) $e + O_2 \to O + O^-$
(19) $O^- + O_2 \to O + O_2 + e$
(20) $O^- + O_2(a^1\Delta_g) \to O_3 + e$
(21) $e + O_2 \to 2e + O_2^+$
(22) $e + O^- \to O + 2e$

bution functions in close agreement with experiments [2]. With the charge exchange cross section given in Ref. [4], on the other hand, we could not reproduce the experimental findings – neither with our PIC-MCC code nor with the BIT1 code [7], which we used to cross-check our results.

For ion-ion neutralization, we employed the cross section of a two-channel Landau-Zener model [8], $\sigma_n(E) = 4\pi R_x^2 \left(1 + \frac{1}{R_x E}\right)$, where R_x is a free parameter which we adjusted to obtain the experimentally measured cross section at high energies [9]. This cross section deviates dramatically from the one used in Ref. [4], but it is based on a clear physical picture for the neutralization process as well as empirical data at high energies.

Detachment of O^- on neutrals occurs through direct detachment (19) and associative detachment (20). The latter is rather surprising because there is no evidence for it in beam experiments [10]. Yet, investigations of O_2 discharges strongly suggest that associative detachment is

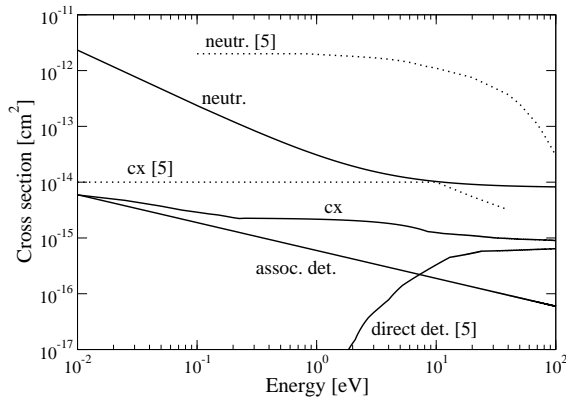Fig. 2: Cross sections for (O_2^+, O_2) charge exchange scattering (9), ion-ion neutralization (17), direct detachment (19), and associative (20) detachment. The dotted lines indicate the respective cross sections used in Ref. [4].

Fig. 3: Cycle-averaged electron and ion density profiles for a rf discharge in O_2 without associative detachment (20) taken into account. The parameters of the discharge are $L = 2.5$ cm, $f = 13.6$ MHz, $p = 13.8$ Pa and $U = 250$ V.

possible because of the presence of metastable $O_2(a^1\Delta_g)$ and may be even the main loss process for O^- in some pressure range [3]. Due to lack of empirical data for this process, we employed a simple model, which describes detachment as the "inverse" of a Langevin-type electron capture into an attractive auto-detaching state of O_3^-. The cross section of which reads

$$\sigma_{ad}^\Delta(E) = 5.96 \cdot \frac{10^{-16} \cdot cm^2}{\sqrt{E[eV]}} \ , \qquad (1)$$

where we assumed the polarizability of $O_2(a^1\Delta_g)$ to be the same as for O_2. Note, in contrast to the cross section for direct detachment, the cross section for associative detachment has no threshold. To determine the probability for this process, we also need the density of $O_2(a^1\Delta_g)$. Within the three species model this density is unknown. It should be however of the order of the O_2 density. As a first step, we write therefore $n_\Delta = C \cdot n_{O_2}$, with $C < 1$ an adjustable fit parameter.

3. Results

Similar to other electro-negative gas discharges, the presence of negative ions in an oxygen discharge leads to abrupt changes in the ion density which, in most cases, forces the discharge to stratify into a quasi-neutral ion-ion and a peripheral electro-positive edge plasma. The details of the stratification depend on the interplay between plasma-chemistry and electrodynamics.

In oxygen discharges two plasma-chemical processes are of particular importance: Ion-ion
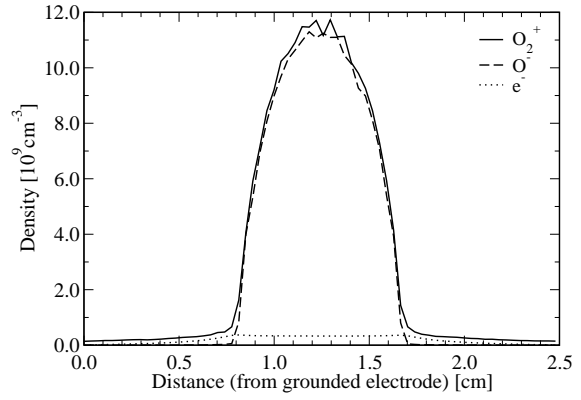
neutralization and associative detachment due $O_2(a^1\Delta_g)$. Although the three species plasma model cannot fully describe associative detachment, because it assumes an homogeneous background of $O_2(a^1\Delta_g)$ molecules, it nevertheless gives clear evidence that the latter process is indispensable for a correct description of experiments.

To demonstrate this, we simulated the discharge of Katsch and coworkers [3]. In Figs. 3 and 4 we show, respectively, the quasi-stationary, cycle-averaged density profiles of the simulated charged particles for $p = 13.8$ Pa, $U = 250$ V, $L = 2.5$ cm, and $f = 13.6$ MHz without and with associative detachment taken into account. The parameter $C \approx 1/6$, implying that one-sixth of the O_2 molecules are in the metastable state. The precise value of C should not be taken too serious because it is based on a rather crude model for associative detachment. More important is that without this process ($C = 0$), the simulation could not reproduce the measured densities.

Whereas the simulation with associative detachment reproduces reasonably well the densities of charged particles in the center of the discharge, the shapes of the (axial) density profiles deviate from the measured ones. Compared to experiment, the central plasma is too narrow, most notably, for lower voltages (not shown here) [1]. This is a shortcoming of the three species plasma model which ignores the spatial dependence of the $O_2(a^1\Delta_g)$ density which, in reality, results from the interplay of volume and surface loss and gen-
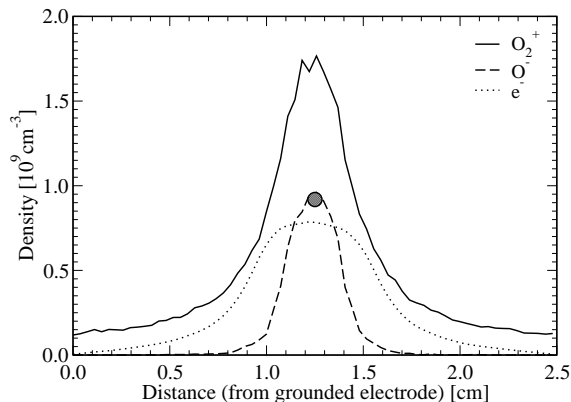
Fig. 4: Same plot as Fig. 3 but now with associative detachment (20) taken into account. Experimentally, $n_e \approx n_{O^-} \approx 0.9 \cdot 10^9$ cm^{-3} (grey bullet) [3].

Fig. 5: Time dependence (for five rf cycles with duration T_{rf}) of the current densities corresponding to the cycle-averaged, quasi-stationary density profiles shown in Figs. 3 and 4, respectively.

eration processes. Because the probability of associative detachment is proportional to n_Δ, the $O_2(a^1\Delta_g)$ density profile should strongly affect the density profiles of charged particles.

In Fig. 5 we finally plot the time-resolved current densities through the discharges shown in Figs. 3 and 4. The current densities are almost the same, irrespective of whether associative detachment is taken into account or not. This is a consequence of the fact that in both cases the main part of the current is carried by the electrons whose densities, in turn, are basically identical. Further studies are needed to reveal if this is an artifact of our model, or if indeed two rather different density profiles are consistent with a given external power supply, $\langle U_{rf} \cdot j_{rf} \rangle_{rf} \cdot A$, where A is the area of the electrodes and $\langle ... \rangle_{rf}$ denotes the cycle average. The configuration realized in the discharge depends then on the plasma-chemistry, in particular, on the outcome of the competition between ion-ion neutralization and associative detachment.

4. Conclusions

We constructed an 1D three-species PIC-MCC model for capacitively coupled rf discharges in oxygen. The model simulates three kinds of charged particles (e, O^-, and O_2^+) and retains neutral particles indirectly via collisions with the simulated charged particles. This is sufficient to reproduce measured central electron and ion densities. However, the (axial) ion density profiles of the simulations are too narrow compared to the experimental ones. We expect better agreement, when the modeling also allows for the possibility
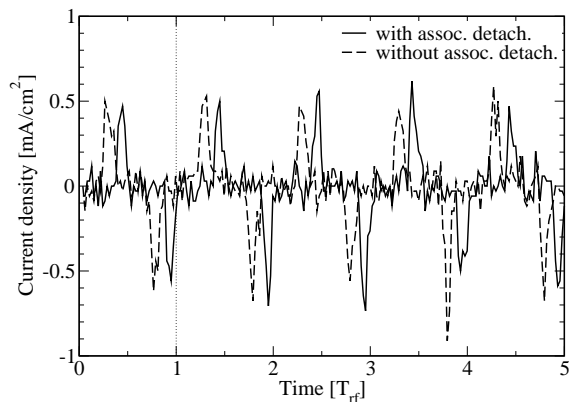
of $O_2(a^1\Delta_g)$ density profiles. For that purpose, the $O_2(a^1\Delta_g)$ molecules, together with their main loss and generation processes, have to be explicitly included in the Monte-Carlo collision approach.

References

[1] F. X. Bronold *et al.*, unpublished.

[2] K. Dittmann *et al.*, unpublished.

[3] H. M. Katsch *et al.*, Plasma Sources Sci. Technol. **9** (2000) 323.

[4] V. Vahedi and M. Surendra, Comput. Phys. Commun. **87** (1995) 179.

[5] R. F. Stebbings *et al.*, J. Chem. Phys. **38** (1963) 2277.

[6] D. R. Gray and J. A. Rees, J. Phys. B **5** (1972) 1048.

[7] D. Tskhakaya and S. Kuhn, Contrib. Plasma Phys. **42** (2002) 302.

[8] R. E. Olson, J. Chem. Phys. **56** (1972) 2979.

[9] R. Padgett and B. Peart, J. Phys. B **31** (1998) L995.

[10] J. Comer and G. J. Schulz, J. Phys. B **7** (1974) L249.